Journal of Pharmacology and Toxicology

ISSN 1816-496X

Academic Journals Inc.

www.academicjournals.com

OPEN ACCESS Journal of Pharmacology and Toxicology

ISSN 1816-496X
DOI: 10.3923/jpt.2025.45.66

Research Article
Effects of Altered K_{2p}, Mid 1 and NALCN Expression on Membrane Potential During Exposure to Various Extracellular K^+ Concentrations

[1]Elizabeth R. Elliott, [1,2]Youngwoo Kim, [3]David Murrugarra and [1]Robin L. Cooper

[1]Department of Biology, University of Kentucky, Lexington, Kentucky 40506, United States of America
[2]The Gatton Academy, 1906 College Heights Blvd. #71031, Bowling Green, Kentucky 42101, United States of America
[3]Department of Mathematics, University of Kentucky, Lexington, Kentucky 40506, United States of America

Abstract

Background and Objective: Two-pore domain potassium (K_{2p}) channels and sodium leak channels (NALCN) are known to play important roles in the maintenance of resting membrane potential through facilitation of, respectively, potassium ion efflux and sodium ion influx across cell membranes. The expression levels of these channels are known to alter under certain pathological conditions-such as diseased/cancerous tissues-so it is of great interest to understand the effects of varied expression for both. This study aims to evaluate how K_{2p} overexpression and RNA interference (RNAi) of Mid1 and NALCN influence membrane potential responses under different extracellular potassium (K) concentrations. **Materials and Methods:** The following *Drosophila melanogaster* lines were used: Two RNAi lines for the knockdown of NA and Mid1, respectively in muscles 6 and 7; UAS lines without altered expression; a line overexpressing a K_{2p} channel subtype; and a line overexpressing nonconducting K_{2p} channels. Each line was exposed to saline solutions containing varied concentrations of potassium and the membrane potential was measured throughout. A minimum of ten preparations were examined in each case. Several lines were also observed with pharmacological alterations. Statistical analysis, performed using Sigma Stat (v15.0), involved expressing data as Mean±SEM, applying paired t-tests or Wilcoxon rank-sum tests (after Shapiro-Wilk normality check), with $p<0.05$ considered significant. **Results:** The results suggest that overexpression of K_{2p} channels increases potassium permeability, as would be expected, which may contribute to the altered activity patterns visible in unhealthy cells. The NALCN knockdown primarily affected responses to lower potassium levels, with significant differences observed only at certain concentrations. Parallel work compared these results to Java simulations of the Goldman-Hodgkin-Katz equation. **Conclusion:** These findings provide an understanding of how cells with overexpression of K_{2p} channels or knockdown of NALCN would behave with changes in external environments or by electrical stimulation.

Key words: NALCN, K_{2p} channel, membrane potential, simulations, pharmacological alterations

Citation: Elliott, E.R., Y. Kim, D. Murrugarra and R.L. Cooper, 2025. Effects of altered K_{2p}, Mid1 and NALCN expression on membrane potential during exposure to various extracellular K^+ concentrations. J. Pharmacol. Toxicol., 20: 45-66.

Corresponding Author: Robin L. Cooper, Department of Biology, University of Kentucky, Lexington, Kentucky 40506, United States of America

Competing Interest: The authors have declared that no competing interest exists.

Data Availability: All relevant data are within the paper and its supporting information files.

INTRODUCTION

Membrane potential is regulated by a combination of pumps, exchangers and channels, which requires well-maintained and highly precise cooperation among these proteins, particularly in early stages of growth and development; however, this coordination is not yet fully understood. Learning more about the regulation of the proteins involved-especially as regards cellular functions for excitation and inhibition-is very important for full understanding of cell physiology. In particular, altered expression of these proteins can have significant effects on the organism as a whole, with linkages to both disease states and pharmacological actions, though it is not yet known whether these changes are cause or consequence of the pathology.

First identified in yeast, the two-pore-domain potassium channel (K_{2p})-also known as the cell's potassium leak channel-is understood to play significant roles in the maintenance of resting membrane potential[1]. Cells are known to have large potassium permeability, which drives the resting membrane potential (RMP) closer to the equilibrium potential for potassium (E_K). It is also known that certain pathological conditions are accompanied by altered K_{2p} channel expression; this has, in particular, been observed in cancerous tissues and other disease states[2]. Cardiac K_{2p} channel overexpression has also been observed to result in decreased heart rate and heightened pH sensitivity, while skeletal overexpression saw a more hyperpolarized resting membrane potential (even closer to E_K) and a greater number of quantal events[3,4].

However, another leak channel might be of investigative interest: Specifically, the sodium leak channel. The NALCN is a nonselective, passive protein channel primarily responsible for a leaky current of Na^+ ions across the cell membrane. In *Drosophila*, NALCN-also referred to as Rb21, VGCNL-1 and NA- is a part of a larger aggregate protein complex known as the NALCN channelosome, which also includes other associated proteins like Mid1[5-7]. For a given cell, the Na^+ influx through NALCN leads to depolarization and, thus, both activation of voltage-gated channels (including but not exclusive to voltage-gated sodium channels) and greater excitability[8]. The NALCNs are responsible for the regulation of rhythmic behavior-such as circadian rhythms and respiration-through alterations in membrane potential for rhythmically firing neurons[9,10]. The action of these channels is not affected by voltage change but can be influenced by neurotransmitters and calcium[9,11].

The NALCN channels are understood to be nonselective and non-inactivating[10]; they are also associated with subunits UNC-79, UNC-80 and NLF-1/FAM155[7], as past research has indicated that mutants bearing loss-of-function alleles for UNC-79 and UNC-80 exhibit defects similar to those observed in organisms lacking the channels entirely[12]. In animals, NALCN channels are believed to be closely related to fungal calcium channels[13]; not only do the functions of both channels rely on accessory proteins, but the NALCN channel itself has also been connected to forms of the Mid1 protein[14,15]. In humans, NALCN is mainly expressed in the central nervous system-largely in neurons, but also in oligodendrocytes and, occasionally, astrocytes-as well as in the heart, adrenal and thyroid glands, lymph nodes and islets of Langerhans[6].

Much like altered K_{2p} channel expression has been connected to widespread pathologies, genes encoding for NALCN may be connected to human pathologies such as bipolar disorder, schizophrenia, Alzheimer's disease, autism, epilepsy, alcoholism, cardiac diseases and cancer[6]. Work has previously been done with model organisms to examine the effects of altered NALCN expression on the organism's physiology. Alterations in NALCN expression result in altered responses to general anesthetics, such as halothane[14-16]. In mice, NALCN knockouts featured primary hippocampal neurons with an RMP hyperpolarized by about 10 mV, suggesting that the depolarizing current from NALCN channels counterbalances the hyperpolarization afforded by K_{2p} channels[10]. While the knockouts developed normally up to 12 hrs after birth, they failed to survive an additional 12 hrs without succumbing to a disrupted respiratory rhythm, and diaphragmatic innervation lacked the rhythmic electrical activity usually observed in wild-type organisms[10]. Knockouts also illustrated sporadic breathing (referring to several seconds of apnea followed by several more of deep breathing) that has been compared to Cheyne-Stokes respiration patterns in humans with central nervous system damage[17]. In *Drosophila melanogaster* organisms bearing genome-wide gene knockouts, fewer viable offspring were born than are observed with wild type[6,14].

Voltage difference across a membrane is usually estimated using the Goldman-Hodgkin-Katz (GHK) equation for ion movement and voltage, which provides an estimate for resting membrane potential that takes into account ion movements/permeabilities[18,19]; however, this equation generally assumes that electric fields remain constant and disregards non-linear factors[20,21]. Modifications to the traditional GHK equation have been used over the years-most notably, the Poisson-Nernst-Planck ion channel models to address ion channel charges and the ionic factors of surrounding media-though the original is still foremost in the field[22-24]. Additionally, factors like ionic passive exchangers or electrogenic pump transport are not considered in either the GHK or the generalized Poisson-Nernst-Planck equations[25],

so users are left to bear in mind that biological cells deviate from these estimates. In theory, however, altering a biological parameter in a well-understood model organism (e.g., changing membrane permeability by inducing abnormal leak channel expression) and then exposing that organism to various driving gradients can allow an examination of the effects on voltage, which may aid understanding of the cell and its functioning.

The model organism used herein was *Drosophila melanogaster*. Not only does this organism allow for effective genetic manipulation to alter channel expression, but it is also a very good model because it is accessible and well-defined for electrophysiological recordings[26]. Additionally, physiological studies generally work well in larval *D. melanogaster* preparations due to good visibility and easy access to nerve terminals at neuromuscular junctions for manipulation[27]. The *Drosophila* E_K has also been estimated to be around -90 mV for larval muscle fibers[11]. Finally, this model also allows for GFP co-expression with K_{2p} channel overexpression through optimization of the lines' genetic construct; it was thus possible to determine whether the conducting and nonconducting dORK channels (i.e., the *Drosophila* equivalent of the K_{2p} channel subtype ORK) were successfully expressed[28-36].

This study utilized genetically modified *Drosophila melanogaster* to investigate how altered expression of K_{2p} and NALCN channels influences resting membrane potential under varying extracellular potassium concentrations, providing preliminary insights into their physiological roles and potential clinical relevance.

MATERIALS AND METHODS

Study area: This research was conducted at the University of Kentucky in Lexington, Kentucky, USA, between May, 2024 and May, 2025.

Animals: *Drosophila melanogaster* Canton S (CS) flies-originally obtained from the Bloomington Drosophila Stock Center (BDSC) but isogenic in the laboratory-were used throughout this investigation. Larvae were used as early third instars (50-70 hrs post-hatching).

Overexpression of the ORK1 protein in larval body wall muscles (m6 and m7) was achieved by crossing homozygous males of BG487 (BDSC stock # 51634) with female virgins of UAS-ORK1 (BDSC stock # 6586). Progeny-referred to as m6m7>ORK1-carried one copy each of the GAL4 driver and UAS-ORK1, resulting in an anteroposterior gradient of BG487-Gal4 expression in body wall muscles 6 and 7[37,38]. Control overexpression of nonconducting K_{2p} channels was obtained by crossing BG487 males with female virgins bearing a non-conducting ORK1 transgene (BDSC stock # 6587); these progeny were referred to as m6m7>non-ORK1. This line also featured GFP co-expression to confirm success[19,20]. Larvae were maintained at room temperature (~21°C) in vials partially filled with a medium of cornmeal, agar, dextrose and yeast.

In addition to the GFP co-expression used to verify successful K_{2p} overexpression, the effectiveness of the Gal4-UAS coordination was verified using an expression of Texas Red to highlight the muscles targeted in the BG487 strain[37]. Muscle 31 in segment 1 had the best channel expression level for this strain of muscle expression, but is rendered hard to preserve by the fact that the dissection process necessary to expose the muscle is complicated; thus, m6 of segment 2 was used instead, as it survived the dissection process more reliably[39].

The NALCN expression was affected using two RNAi lines; homozygous males of BG487 (BDSC stock # 51634) were crossed with virgin females of Mid1 RNAi (BDSC stock # 36754) and NA RNAi (BDSC stock # 25808) to yield progeny referred to, respectively, as m6m7>Mid1 RNAi and m6m7>NA RNAi flies. BG487-GAL4 (larval body wall muscles m6 and m7 in an anteroposterior gradient in larval body wall muscles 6/7). Larvae were maintained in vials partially filled with a cornmeal-agar-dextrose-yeast medium and maintained at room temperature (~21°C).

Physiological recordings: The dissection procedures and electrophysiological measures reported herein are very similar to those previously described by Elliott and Cooper[39]. Sharp intracellular electrodes (30 to 40 megaOhm resistance) filled with 3 M KCl were used to measure transmembrane potentials in m6 muscles of early third-instar larvae. An Axonclamp 2B (Molecular Devices, Sunnyvale, California, USA) amplifier and 1×LU head stage were used, while data were collected and analyzed in LabChart 7.0 (ADInstruments, Colorado Springs, Colorado, USA). Exposure time was kept to three minutes unless the membrane potential had not stabilized and more time was needed.

The dissection saline was haemolymph-like 3(HL3): 70 mM NaCl, 5 mM KCl, 20 mM MgCl2·6H2O, 10 mM NaHCO3, 5 mM Trehalose, 115 mM sucrose, 25 mM BES and 1 mM $CaCl_2 \cdot 2H_2O$, kept at pH 7.2[40,41]. Monitoring of the pH was conducted using an Accumet model 10 pH meter (Fisher Scientific). Experimental salines featured varied KCl as described in the results section.

Appendix 1: Parameters used for coding the GHK estimations

For running the GHK Equation to estimate equilibrium potentials the GitHub code was used:
https://github.com/ywkim17/Educational_Book/blob/main/GHK.py.
The code named "GHK.py" was run on the VSCode software.

```
import math
def ghk(R, T, F, P_K, K_in, K_out, P_Na, Na_in, Na_out, P_Cl, Cl_in, Cl_out):
&amp;quot;&amp;quot;&amp;quot;
Computes membrane potential (Vm) in millivolts using the Goldman-Hodgkin-Katz equation.
```

Parameters

R	:	Float-Universal gas constant (J/(mol·K))
T	:	Float-Temperature in Kelvin (K)
F	:	Float-Faraday's constant (C/mol)
P_K	:	Float-Permeability of potassium
K_in	:	Float-Intracellular potassium concentration (mM)
K_out	:	Float-Extracellular potassium concentration (mM)
P_Na	:	Float-Permeability of sodium
Na_in	:	Float-Intracellular sodium concentration (mM)
Na_out	:	Float-Extracellular sodium concentration (mM)
P_Cl	:	Float-Permeability of chloride
Cl_in	:	Float-Intracellular chloride concentration (mM)
Cl_out	:	Float-Extracellular chloride concentration (mM)
P_Ca	:	Float-Permeability of calcium
Ca_in	:	Float-Intracellular calcium concentration (mM)
Ca_out	:	Float-Extracellular calcium concentration (mM)

Returns

```
Vm (float): Membrane potential in millivolts (mV)
&amp;quot;&amp;quot;&amp;quot;
# Calculate RT/F in millivolts
V_T = (R*T)/F*1000 # Convert to mV
numerator = (P_K*K_out+P_Na*Na_out+P_Cl*Cl_in)
denominator = (P_K*K_in+P_Na*Na_in+P_Cl*Cl_out)
if denominator == 0:
raise ValueError(&amp;quot;Denominator is zero; check input values.&amp;quot;)
Vm = V_T*math.log(numerator/denominator)
return Vm
# Parameter Inputs
R = 8.314 #Constant Value
T = 294.15
F = 96485 #Constant Value
P_K, K_in, K_out = 1.3, 140, 220
P_Na, Na_in, Na_out = 0.001, 15, 10
P_Cl, Cl_in, Cl_out = 0.8, 10, 110
# Compute membrane potential
Vm = ghk(R, T, F, P_K, K_in, K_out, P_Na, Na_in, Na_out, P_Cl, Cl_in, Cl_out)
print(f&amp;quot;\nmembrane potential: {Vm:.2f} mV&amp;quot;)
```

The initial values for starting the simulations for the larval Drosophila muscle were as shown below:

The saline used for larval Drosophila physiological measures is: (in mmol/L) 70 NaCl, 5 KCl, 20 $MgCl_2$, 10 $NaHCO_3$, 1 $CaCl_2$, 5 trehalose, 115 sucrose, 25 N,N-bis(2-hydroxyethyl)-2-aminoethane sulfonic acid (BES) and pH at 7.2.

[K+]i	=	190 mM (estimated for Drosophila muscle)
[K+]o	=	5 mM (Saline)
[Na+]i	=	12 mM (assume for Drosophila muscle)
[Na+]o	=	80 mM (Saline)
[Cl-]i	=	12 mM (assume for muscle)
[Cl-]o	=	91 mM
pK	=	1 (assume for muscle)
pNa	=	0.001 (assume for muscle)
pCl	=	0.01 (assume for muscle)

Salines containing NMDG featured the compound at a concentration of 70 mM to replace the Na^+ in solution by NaCl; although 10 mM $NaHCO_3$ remained in this altered saline. All chemicals were from Sigma-Aldrich (St. Louis, Missouri, USA). It is important to note that the pH of the NMDG-containing salines was kept at the same pH as the other salines (7.2) and that the NMDG was added to be equimolar with the amount of NaCl removed. The pH was very stable in the modified HL3 saline used, as it contained 25 mM BES buffer; thus, the NMDG is likely a Cl^- form (i.e., NMDG-Cl). For the CP-96345 studies, 1.0 mg CP-96345 (Tocris Bioscience; Minneapolis, Minnesota, USA) was dissolved in 50 µL DMSO before adding 50 mL of warmed saline, yielding a 50 µM solution. All other chemicals were obtained from Sigma-Aldrich (St. Louis, Missouri, USA).

GHK simulations: To program the simulation, a Python-integrated environment (i.e., Python extension of the VSCode platform) and two GitHub codes (https://github.com /ywkim17/Educational_Book/ blob/main/Nernst.py and https://github.com/ywkim17/Educational_Book/blob/main/GHK.py) were used. The codes named "Nernst.py" and "GHK.py" (Appendix 1) were used via the VSCode software.

Statistical methods: Statistical analysis was conducted using the same methods as previously described by Lu *et al.*[10]. In brief, data are expressed as averages (Mean±Standard Error). Paired t-tests were used to quantify response differences before and after solution exchange, while normality was established using the Shapiro-Wilk test and, when appropriate, the Wilcoxon rank sum, non-parametric test was used. Analysis was conducted using Sigma Stat software (version number 15.0), with $p<0.05$ being considered statistically significant.

Ethical consideration: Invertebrate animal care was approved by the Institutional Animal Care and Use Committee.

RESULTS

Using the m6 muscle provides an easily identifiable and accessible muscle with a relatively simple dissection; however, exposing m6 in segment 2 requires extra care to avoid damage when removing the larval CNS. The larvae were checked for m6 GFP expression just before recordings to ensure the success of the K_{2p} overexpression in these muscles. As shown in Fig. 1, an anterior-posterior expression gradient and well-defined m6 and m7 were observed. Identification of m6 and m12 was performed in segment 2, as this process is relatively easy with electrophysiological recordings (Fig. 1a-b). Only white light (i.e., not fluorescent imaging) was used for electrode placement, as m6 was easily identifiable.

Membrane potential measured during exposure of representative fibers to a series of raised $[K^+]_o$ in m6m7>ORK1 (Fig. 2) and m6m7>non-ORK1 (Fig. 3) larvae was observed to reach fairly level states within two minutes of exposure to a new $[K^+]_o$, at which point reliable measurements could be taken. The x-axis of each recording represents time (as per the key) and is marked with the solution concentrations (mM) present at each point in the recording; the y-axis of each reports membrane potential (mV).

Figure 4 compares the resting membrane potential responses of m6m7>non-ORK1 and m6m7>ORK1 *Drosophila* preparations across a range of extracellular potassium concentrations. Larvae overexpressing non-conducting K_{2p} channels maintained a potential of approximately -55 mV at 0 mM $[K^+]_o$, showing only a slight depolarization with

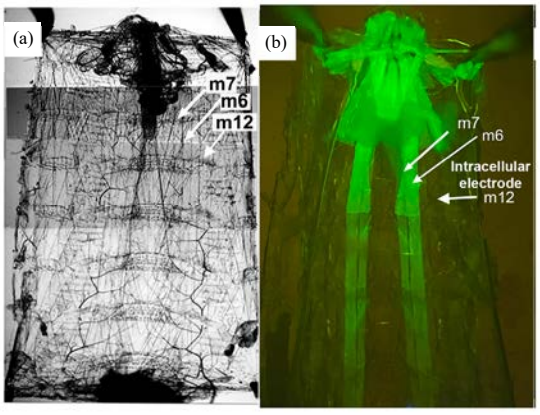

Fig. 1(a-b): *Drosophila* preparation dissected for selective *in situ* recording of muscle membrane potential in early 3rd instar larvae with m6m7>ORK1 and GFP co-expression, (a) Intracellular recording view showing muscles 6, 7, and 12 in segment 2 and (b) GFP expression in muscles 6 and 7 of BG487-GAL4 larvae, highlighting the anteroposterior gradient

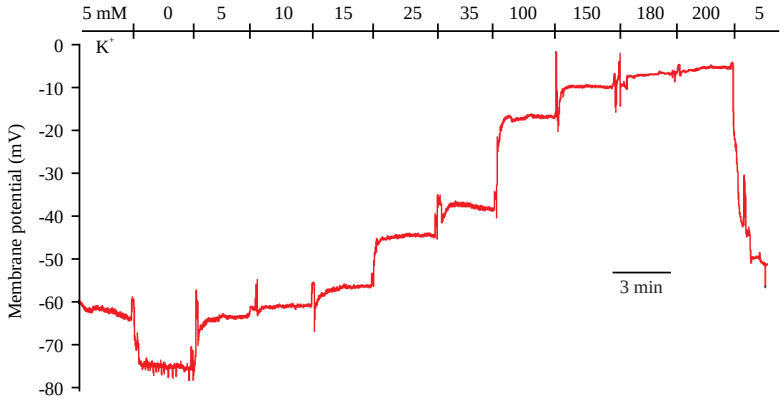

Fig. 2: A representative trace of the membrane potential obtained from a m6m7>ORK1 preparation observed under conditions of varied extracellular potassium

Solution exchange for potassium level alteration was performed as marked along the upper axis, with the exchange resulting in occasional trace artifacts (visible as deflections on the recording)

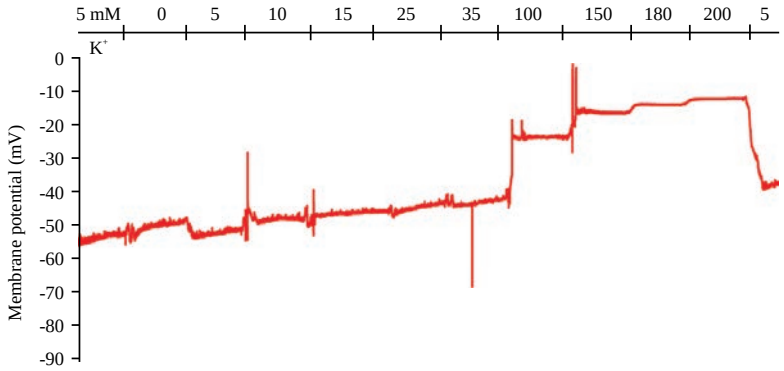

Fig. 3: A representative trace obtained from a m6m7>non-ORK1 preparation observed under conditions of varied extracellular potassium

Solution exchange for potassium level alteration was performed as marked along the upper axis, with the exchange resulting in occasional trace artifacts (visible as deflections on the recording)

increased $[K^+]_o$. In contrast, larvae overexpressing conducting K_{2p} channels exhibited a more hyperpolarized resting potential (~-80 mV at 0 mM $[K^+]_o$) and a much steeper depolarization as $[K^+]_o$ rose, reflecting heightened potassium sensitivity. Overall, the m6m7>ORK1 and m6m7>non-ORK1 preparations responded to the $[K^+]_o$ series in a fairly consistent manner (Fig. 4a-b). On the whole, m6m7>ORK1 larvae featured more negative membrane potentials at 5 mM $[K^+]_o$ as compared to the m6m7>non-ORK1 strain ($p<0.05$, t-test, $n = 10$). The differences in the two strains are more obvious in enlarged graphs of lower concentration responses (Fig. 5), with significant differences indicated at concentrations of 0, 5, 10 and 15 mM ($p<0.05$, t-test for each equal concentration $[K^+]_o$ compared between the strains; $n = 10$).

Semi-logarithmic plots demonstrate a linear relationship between membrane potential and raised $[K^+]_o$; however, these plots cannot include data from 0 mM $[K^+]_o$ (Fig. 6a-b). The m6m7>ORK1 ($R^2 = 0.9944$) strain revealed a tighter linear relationship than m6m7>non-ORK1 ($R^2 = 0.9584$). At 25 mM $[K^+]_o$ and higher concentrations, no further differences in membrane potential were revealed between the lines, so the linear relationships for these concentrations were equal.

The responses observed in the NALCN control lines (UAS-Mid1 and UAS-NA) underwent similar trends to those targeted with NA-RNAi and Mid1-RNAi when exposed to alteration of external K^+ concentration (i.e., $[K^+]_o$); as $[K^+]_o$ was increased, membrane potential was observed to depolarize, as demonstrated in the representative traces included (Fig. 7a-e). Lower $[K^+]_o$ exposure resulted in relatively stable recordings,

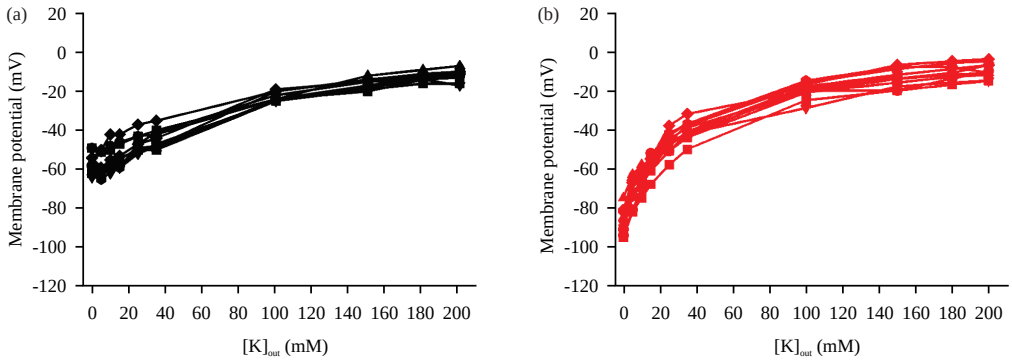

Fig. 4(a-b): Summary graphs comparing m6m7>non-ORK1 (non-conducting K_{2p}) and m6m7>ORK1 (conducting K_{2p}) responses to increasing extracellular potassium concentrations, (a) Non-conducting K_{2p} overexpression maintained a resting membrane potential of -55 mV at 0 mM $[K^+]_o$, showing only a gradual depolarization with rising $[K^+]_o$ and (b) Conducting K_{2p} overexpression produced a more hyperpolarized resting potential (-80 mV at 0 mM $[K^+]_o$), followed by a markedly steeper depolarization as $[K^+]_o$ increased

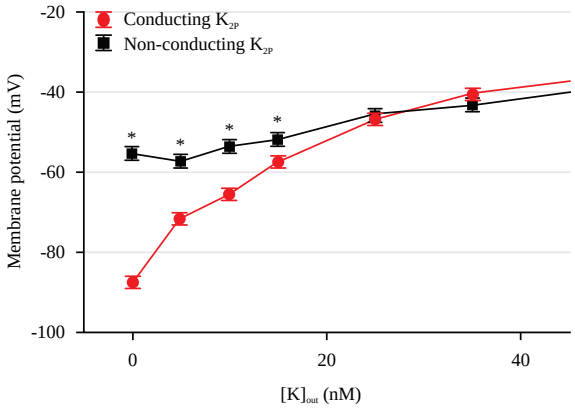

Fig. 5: Comparison of the average trends observed with varied extracellular potassium in preparations
Overexpressing conducting (m6m7>ORK1) and non-conducting (m6m7>non-ORK1) K_{2p} channels are shown, with significant differences illustrated at potassium concentrations of 0, 5, 10, and 15 mM, *p<0.05, t-test and n = 10

while switching the bathing media from 35 mM $[K^+]_o$ to 100 mM $[K^+]_o$ usually resulted in muscle fiber contraction, including potential dislodging of the microelectrode; however, after the muscles stabilized in that contracted state, the electrode could be reinserted, after which point intracellular recordings could be effectively maintained (as further increases in $[K^+]_o$ i.e., 150 mM through 220 mM-would not induce further contractions). Generally, exchange of the bathing medium back to 5 mM $[K^+]_o$ would cause the muscle to slowly relax, sometimes even slowly enough that the electrode could remain in the fiber throughout the process (i.e., without needing to remove and reinsert the electrode). In most cases, a return to 5 mM $[K^+]_o$ resulted in a return to the more hyperpolarized membrane potentials observed earlier in the series. The m6m7>Mid1 RNAi line was observed via two main methods; membrane potential was observed in the experimental muscle 6 (m6m7>Mid1 RNAi-m6) and in an internal control muscle with normal expression (m6m7>Mid1 RNAi-m12) for within-preparation comparison (Fig. 7d-e).

Potentials were observed under conditions of varied extracellular potassium. The solution exchange for concentration of K^+ was performed as marked along the upper axis, with the exchange resulting in occasional trace artifacts (visible as deflections on the trace). Bars across the traces in A, C and E indicate the level in which the measures were made and assumed to be representative for the effect of $[K^+]_o$.

Variations were observed in resting membrane potential among the preparations, but averaging the recordings made it clear that the Mid1-RNA line differed from the others only over lower $[K^+]_o$, matching the other lines at higher $[K^+]_o$

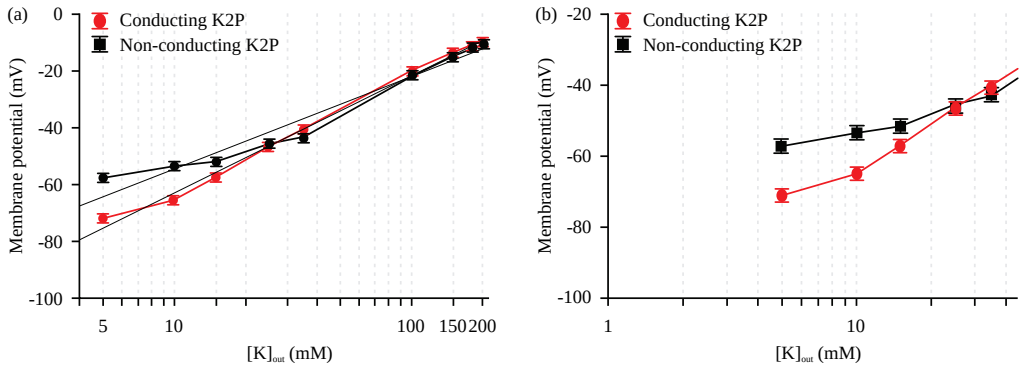

Fig. 6(a-b): Comparison of responses to varied extracellular potassium concentrations in preparations overexpressing conducting (m6m7>ORK1) and non-conducting (m6m7>non-ORK1) K_{2p} channels, (a) Nonlinear regression models fitted to data from both strains, with $R^2 = 0.9584$ for m6m7>non-ORK1 and $R^2 = 0.9944$ for m6m7>ORK1 and (b) Enlarged view of panel A focusing on lower $[K^+]_o$ concentrations to highlight differences between the two regression curves

values (Fig. 8a). For example, the individual datapoints are very spread out at lower concentrations (e.g., 0 mM $[K^+]_o$), while exposure to 100 mM $[K^+]_o$ consistently resulted in a membrane potential of around -20 mV. These differences are more pronounced/visible in a semi-log plot (Fig. 8b).

To better view the differences among lower and higher $[K^+]_o$ data for the various genetic lines, the plots are enlarged (Fig. 9a-b). No differences were observed among the genetic lines for high levels of $[K^+]_o$, but the data at lower $[K^+]_o$ indicate overlapping values for m6m7>NA, UAS-Mid1, UAS-NA and m6m7>Mid1-m12 preparations, while m6m7>Mid1-m6 featured a more negative resting membrane over a range of 0 to 35 mM $[K^+]_o$.

When comparing the lines, the following results were observed (Table 1): UAS-Mid1 preparations had membrane potentials significantly different from m6m7>mid1-m6 ($p<0.05$, ANOVA, n = 6 for each line) at 10 , 15 and 25 mM. Additionally, m6m7>Mid1-m6 was observed to be significantly different from both UAS-NA and m6m7>NA at 35 mM $[K^+]_o$.

Both m6m7>NA-RNAi and m6m7>Mid1-RNAi preparations were expected to show similar responses to varied $[K^+]_o$, as both involved reduced NALCN channel expression, so these two lines were compared over the full $[K^+]_o$ range (Fig. 10). They were observed to be significantly different from each other at 10, 15, 25 and 35 mM ($p<0.05$, t-test for each concentration, n = 6).

To determine how pNa influences the relationship between $[K^+]_o$ and membrane potential, saline Na^+ was replaced with NMDG for the full series of altered $[K^+]_o$ and the effects observed in both the m6m7>non-ORK1 and m6m7>ORK1 larvae (Fig. 11a-b). The relationship between mean membrane potentials in the m6m7>non-ORK1 and m6m7>ORK1 strains appears similar to that observed with Na^+ present in the bathing media; namely, the m6m7>ORK1 larvae had more hyperpolarized membrane potentials at lower $[K^+]_o$ values (Fig. 11c-d). Significant differences were observed (and marked on the graphs below) at concentrations of 0, 5, 10 and 15 mM K^+ ($p<0.05$, t-test for each equal concentration $[K^+]_o$ compared between the strains; n = 10), which are the same concentrations as those exhibiting significant differences when Na^+ was present.

It was expected that reduced $[Na^+]_o$ would result in a more hyperpolarized state at each $[K^+]_o$ examined; however, a more depolarized relationship was observed from 0 $[K^+]_o$ to 100 mM $[K^+]_o$ instead. These more depolarized states were observed in both m6m7>ORK1 and m6m7>non-ORK1 larvae, and are also observed in semi-log plots for both the full distribution and lower $[K^+]_o$ (Fig. 12a-b).

To examine the putative actions of CP-96345 as a NALCN blocker, m6m7>Mid1-RNAi and m6m7>NA-RNAi preparations underwent the full $[K^+]_o$ series while exposed to 50 µM CP-96345 solution. Three other lines were also used to determine whether membrane potential would be affected by CP-96345 exposure: The m6m7>ORK1 line (bearing K_{2p} channel overexpression and the resulting hyperpolarized membrane)[4]; the m6m7>ORK1-NC line (bearing overexpression of non-conducting K_{2p} channels as a control for against protein overexpression and insertion) and a UAS-ORK1 line for comparison. Given that CP-96345 is not water-soluble, DMSO was used to dissolve CP-96345 before adding it to the saline (per manufacturer recommendation) and control experiments were performed to determine the effects of DMSO alone (by exposing the m6m7>NA-RNAi line

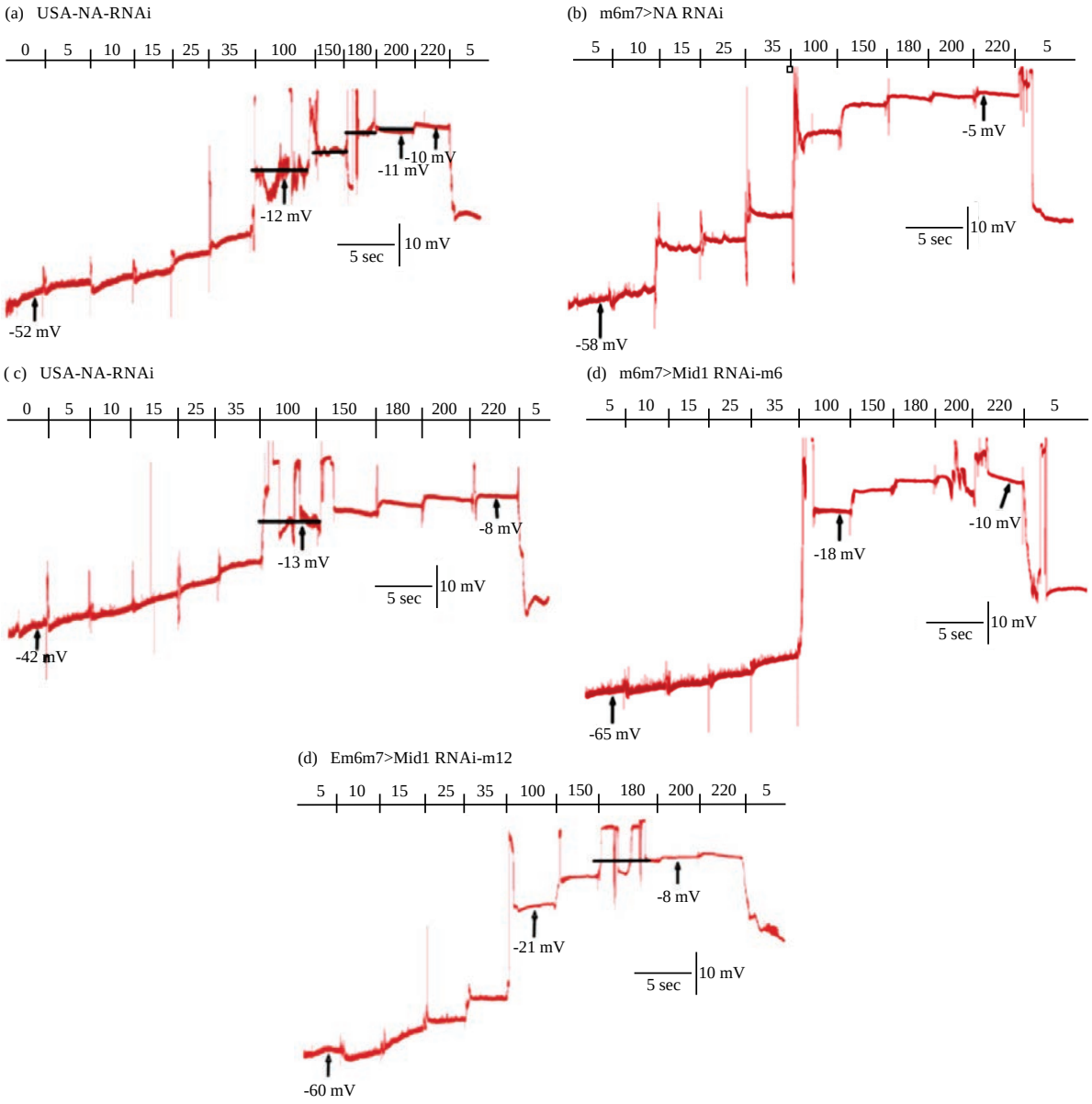

Fig. 7(a-e): Representative traces of membrane potentials obtained from third-instar larvae of RNAi-altered strains: (a) UAS-NA, (b) m6m7>NA, (c) UAS-Mid1, (d) m6m7>Mid1-m6 and (e) m6m7>Mid1-m12
y-axis scale is the same as in Fig. 3 for membrane potential

to DMSO at the same concentration as used for dissolving the CP-96345). All lines were also exposed to a DMSO-saline solution before exposure to the CP-96345-DMSO-saline solution.

As observed in Fig. 13a, all the lines depolarized over time, save the m6m7>ORK1 line, which remained at a relatively stable, more negative potential. This is likely because higher K_{2p} channel expression drives the membrane potential towards the equilibrium potential for K^+. However, unexpectedly, CP-96345 resulted in spontaneous EJPs for some preparations, a response not observed with exposure to DMSO alone (Fig. 13b). These spontaneous events appeared to be caused by random, spontaneous excitation of the nerve.

To estimate the GHK parameters-namely, differences in ionic permeabilities (particularly pK and pNA) between the larval strains-simulations were performed. The external concentrations of K^+, Na^+ and Cl^- ions could be determined through knowledge of the salines' make-ups, but internal concentrations could only be estimated, as was done for earlier studies. The simulation parameters shown in Fig. 7 provided close fits for individual regions of the linear relationship between $[K^+]_o$ and membrane potential in

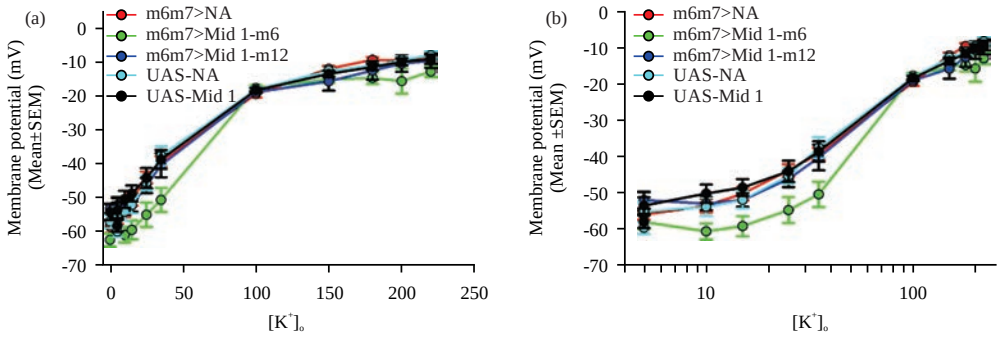

Fig. 8(a-b): Comparison of the average trends observed with varied extracellular potassium in third-instar larvae of RNAi-altered strains, (a) Results of the various RNAi-altered strains are shown: UAS-NA, m6m7>NA, UAS-Mid 1, m6m7>Mid 1 in m6, and m6m7>Mid 1 in m12 and (b) Comparison of the average (±SEM, n = 6) trends observed under the same conditions but graphed on a logarithmic scale

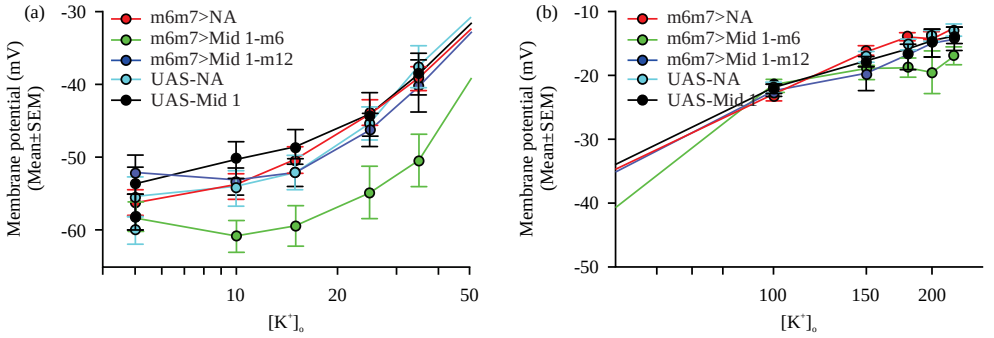

Fig. 9(a-b): Enlarged views of the plots for membrane potential over the range of $[K^+]_o$, (a) Lower 0-35 mM $[K^+]_o$ and (b) Higher 100-220 mM $[K^+]_o$

Same graphs were shown in Fig. 3

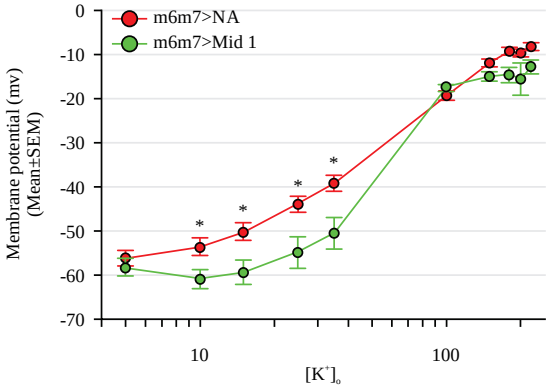

Fig. 10: Average effects of altered extracellular K^+ on membrane potential in strains m6m7>NA and m6m7>Mid 1

Average data of the strains were found to be significantly different from each other at K^+ concentrations of 10, 15, 25 and 35 mM ($p<0.05$, T-test, n = 6)

m6m7>non-ORK1 (non-conducting, Fig. 14a) larvae. Trials were conducted with variations of only pK and pNa estimates, resulting in close matches between empirical and simulated data (Fig. 14a). The closest match was obtained using the parameters specified in simulation number three, which displays permeability variation as the membrane depolarizes. Additional simulations were then performed to determine the parameters that resulted in the empirically obtained

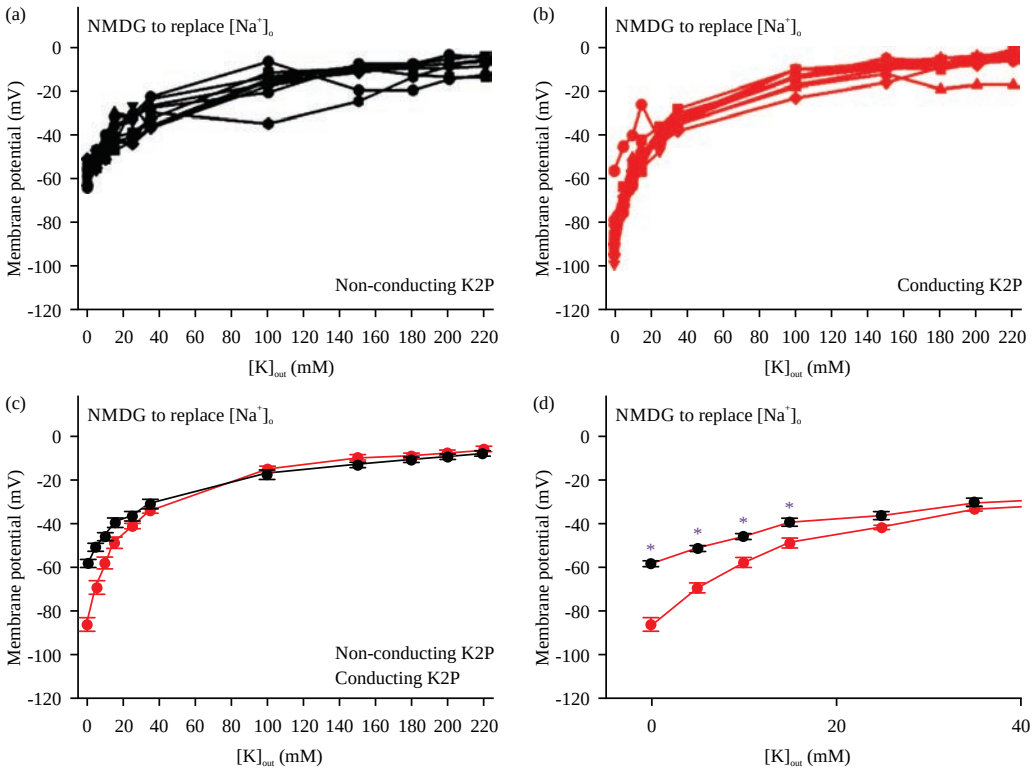

Fig. 11(a-d): Summary graphs of responses to potassium alteration in individual preparations and averaged trends, (a) Non-conducting (m6m7>non-ORK1) K_{2p} channels and (b) overexpressing line (m6m7>ORK1) after replacement of environmental Na^+ with NMDG, (c) Averages (±SEM) of the two lines and (d) An enlarged view for the lower concentrations of $[K^+]_o$

Table 1: Statistical comparison for each group within a concentration of K^+ compared among strains

10 mM	UAS-Mid 1	UAS-NA	m6m7>Mid 1-m6	m6m7>Mid 1-m12	m6m7>NA
UAS-Mid 1	x	x	p = 0.014	x	x
UAS-NA	x	x	x	x	x
m6m7>Mid 1-m6	x	x	x	x	x
m6m7>Mid 1-m12	x	x	x	x	x
m6m7>NA	x	x	x	x	x
15 mM					
UAS-Mid 1	x	x	p = 0.02	x	x
UAS-NA	x	x	x	x	x
m6m7>Mid 1-m6	x	x	x	x	x
m6m7>Mid 1-m12	x	x	x	x	x
m6m7>NA	x	x	x	x	x
25 mM					
UAS-Mid 1	x	x	p = 0.046	x	x
UAS-NA	x	x	x	x	x
m6m7>Mid 1-m6	x	x	x	x	x
m6m7>Mid 1-m12	x	x	x	x	x
m6m7>NA	x	x	x	x	x
35 mM					
UAS-Mid 1	x	x	p = 0.022	x	x
UAS-NA	x	x	p = 0.012	x	x
m6m7>Mid 1-m6	x	x	x	x	x
m6m7>Mid 1-m12	x	x	x	x	x
m6m7>NA	x	x	p = 0.031	x	x

A two-way ANOVA was used for each group of K^+ concentrations, followed by an all pairwise multiple comparison procedure (Holm-Sidak method, n = 6) and x: Statistical testing indicated no significant difference

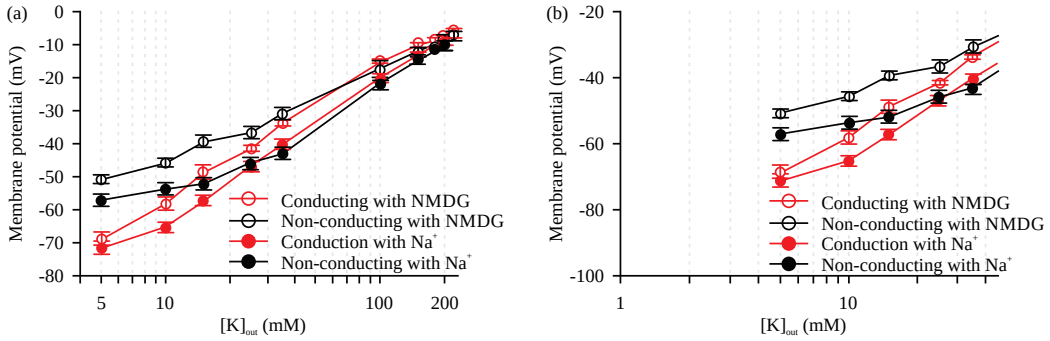

Fig. 12(a-b): Effects of replacing environmental NaCl with NMDG on responses to altered extracellular potassium, (a) Summary graphs comparing m6m7>ORK1 (conducting K_{2p}) and m6m7>non-ORK1 (non-conducting K_{2p}) lines, with and without NaCl replacement by NMDG and (b) Enlarged view of panel A focusing on lower $[K^+]_o$ concentrations to highlight differences between conditions

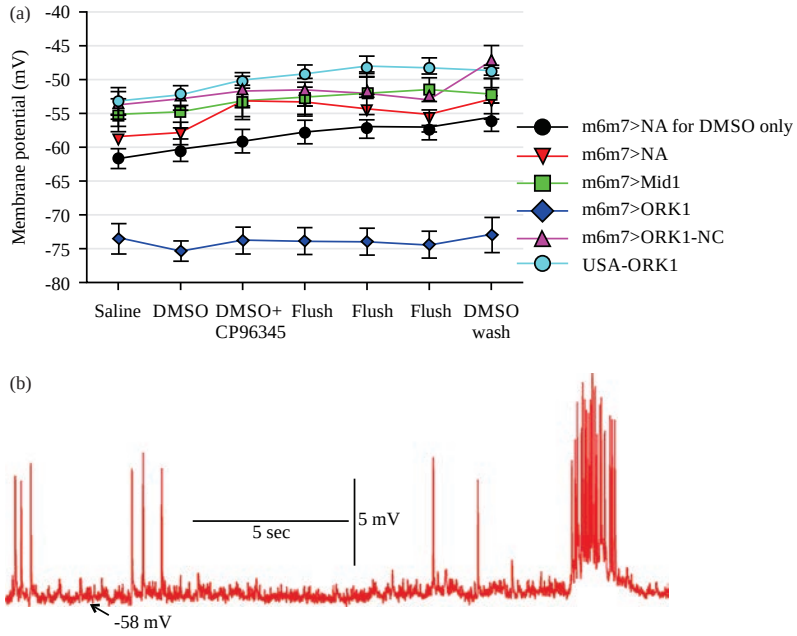

Fig. 13(a-b): Effects of CP-96345 exposure on membrane potential in third instar larvae of m6m7>NA, m6m7>ORK1, m6m7>ORK1-NC and UAS-ORK1 strains, (a) Mean ±SEM; n = 6) membrane potentials recorded over time for each strain under various exposures, including solvent control (DMSO) and DMSO-to-DMSO exchanges to account for solution exchange effects and (b) Representative trace from an m6m7>NA preparation showing CP-96345-induced spontaneous excitatory junction potentials

membrane potential at each step in the series, which involved using a constant pCl estimate and varying both pNa and pK (Fig. 14b).

Prior to comparing the m6m7>ORK1 and m6m7>non-ORK1 larvae, it was expected that the parameter differing most widely would be pK (given that m6m7>ORK1 larvae have greater K_{2p} channel expression); however, the act of increasing only pK did not provide a good fit and pNa had to be increased as well (Fig. 15a). In Fig. 15a, the empirical data (dotted line) could not be achieved through any single parameter set, though the second simulation (green line) was closest over the full $[K^+]_o$ range. These parameters were then fine-tuned until each point in the series matched the datum measured at that concentration, largely through variation in pCl, pNa and pK (Fig. 15b).

Given the depolarized states observed with exposure to NMDG-containing saline, more GHK simulations were conducted to determine the expected membrane potential

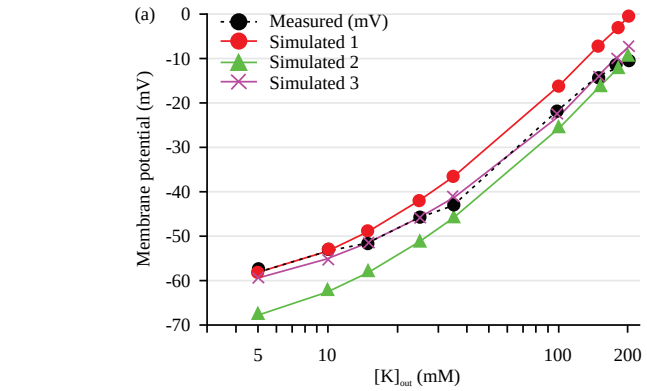

	Sim-1	Sim-2	Sim-3
pk	0.6	0.27	0.3
pNa	0.04	0.001	0.02
pC_i	0.45	0.45	0.45
$[K]_i$	140	140	140
$[Na]_i$	15	15	15
$[Cl]_i$	10	10	10
$[Na]_o$	145	145	145
$[Cl]_o$	110	110	110

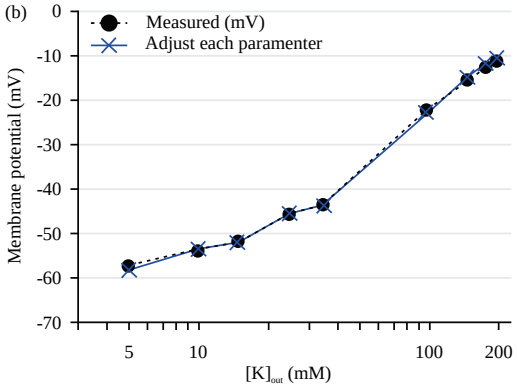

pk	$[K]_i$	pNa	$[Na]_i$	$[Na]_o$	pC_i	$[Cl]_i$	$[Cl]_o$	$[K]_o$
0.6	140	0.04	15	145	0.45	10	100	5
0.6	140	0.04	15	145	0.45	10	100	10
0.6	140	0.025	15	145	0.45	10	100	15
0.6	140	0.02	15	145	0.45	10	100	25
0.3	140	0.02	15	145	0.45	10	100	35
0.3	140	0.02	15	145	0.45	10	100	100
0.3	140	0.02	15	145	0.45	10	100	150
0.3	140	0.001	15	145	0.45	10	100	180
0.27	140	0.001	15	145	0.45	10	100	200

Fig. 14(a-b): Estimated parameters for modeling the relationship between altered $[K^+]_o$ and membrane potential in the m6m7>non-ORK1 strain, (a) Three simulations with varied pNa and pK values overlaid on empirical data (dotted line), with the closest fit achieved in simulation three (purple line) and (b) Adjusted pNa and pK values for each $[K^+]_o$ concentration to match the measured membrane potentials

Corresponding parameter values for panels A and B are listed in the tables to the right

response to reduced NaCl would be. Lines of best fit were also created for the empirical data to allow estimation of how pNa had varied from the expected.

The m6m7>non-ORK1 larvae were observed to produce greater depolarization over the whole $[K^+]_o$ range with removal of NaCl and replacement with NMDG, which was far from expected (Fig. 16a-c). The data obtained for m6m7>non-ORK1 in the presence of NaCl (dotted black line) and without NaCl (purple line) were compared to the simulated distribution without NaCl (blue line). Note that, at 5 mM $[K^+]_o$, the difference between the simulated value and the value measured in the absence of NaCl was measured to be ~17.3 mV, while that between the simulated value and the value measured with NaCl present was only ~6.4 mV (Fig. 16a). It should be noted that increasing KCl in the bath also resulted in altered $[Cl^-]_o$, which would then have increased along with the KCl; this could have altered the resting membrane potential. The $[Cl^-]_o$ alteration was thus incorporated into the simulations conducted (red line in Fig. 16a). The resulting simulated values approached the measured values (purple line) at lower $[K^+]_o$ but not at higher $[K^+]_o$, so additional simulations were performed. The measured values were successfully approximated in three segments (shown in green with labels; Fig. 16a), each with varied parameters to achieve the best possible match. The simulated parameters for these three segments, the values expected with removal of NaCl and the effects of altered $[Cl^-]_o$ are shown (Fig. 16b).

The same approaches were used to estimate expected results for the m6m7>ORK1 larvae exposed to rising $[K^+]_o$ after removal of NaCl and replacement with NMDG, with and without consideration of altered $[Cl^-]_o$ (Fig. 17a-c). Changes in $[Cl^-]_o$ as a result of increased KCl only slightly offset the simulation curve; two attempts were made to estimate the effects of altered $[Cl^-]_o$ (depicted as green triangles; Fig. 17a-c) and both fit the observed data relatively well (purple line). Simulations of the expected values for NaCl replacement without consideration of $[Cl^-]_o$ alterations (blue line) featured

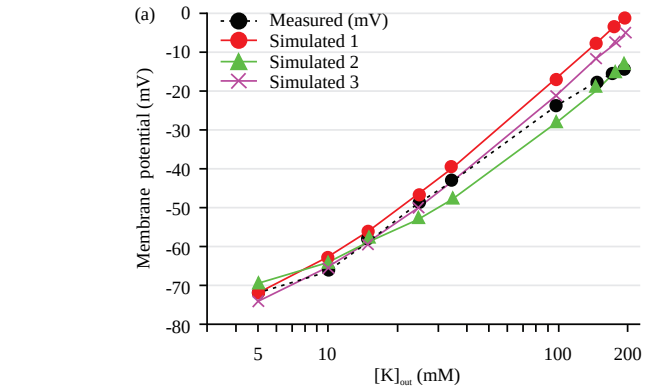

	Sim-1	Sim-2	Sim-3
pk	1.3	0.8	1.3
pNa	0.02	0.001	0.002
pCl	0.4	1.2	0.8
[K]i	140	140	140
[Na]i	15	15	15
[Cl]i	10	10	10
[Na]o	145	145	145
[Cl]o	110	110	110

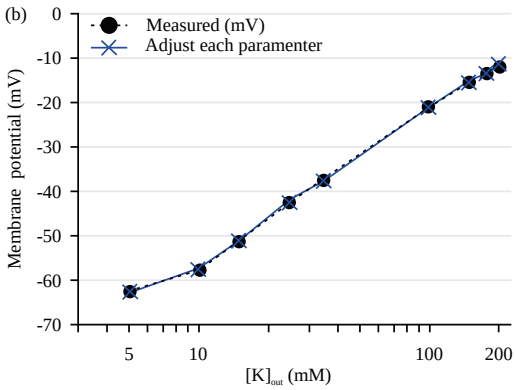

pk	$[K]_i$	pNa	$[Na]_i$	$[Na]_o$	pC_i	$[Cl]_i$	$[Cl]_o$	$[K]_o$
1.3	140	0.02	15	145	0.4	10	100	5
1.3	140	0.004	15	145	0.4	10	100	10
1.3	140	0.001	15	145	0.4	10	100	15
1.3	140	0.001	15	145	0.4	10	100	25
1.3	140	0.001	15	145	0.8	10	100	35
1	140	0.001	15	145	1	10	100	100
0.8	140	0.001	15	145	1	10	100	150
0.8	140	0.001	15	145	1.2	10	100	180
0.8	140	0.001	15	145	1.2	10	100	200

Fig. 15(a-b): Estimated parameters for modelling of the measured relationship between altered $[K^+]_o$ and membrane potential in the m6m7>ORK1 strain, (a) Three different simulations with varied pNa and pK superimposed over empirical values (dotted line). The closest match was obtained with simulation two (green line) and (b) Adjustments of pNa, pK, and pCl at each of the $[K^+]_o$ concentrations to obtain the measured membrane potential

The parameter values obtained for each figure are written in the rightwards tables

more hyperpolarized values than those measured (purple line) but resembled the responses observed with normal [NaCl] (black dotted line) at low $[K^+]_o$.

The simulation parameters that best matched the empirical data obtained for the m6m7>NA RNAi strain are shown in Fig. 18. No one simulation perfectly matched the data, so fragmented simulations were used to obtain close fits between the full range of $[K^+]_o$ exposure and the measured membrane potentials. Trials were conducted with only pK and pNa values varying, resulting in close matches between empirical and simulated data (Fig. 18); indeed, the closest matches were obtained with simulations wherein the pK and pNa values decreased as the membrane depolarized.

Estimates of the GHK parameters for the m6m7>MID1 RNAi strain were also best determined through discrete, fragmented simulations, as membrane potential did not respond to increasing $[K^+]_o$ with the linear increase expected. Two estimates were made, where simulation 2 fits well for the midrange between 35 and 100 mM $[K^+]_o$ and simulation 3 estimated the empirical data around 100 mM $[K^+]_o$. Attempts to address pCa, internal calcium and external calcium were also used, but could not achieve good fits over a full range; the best simulation to estimate the full range (i.e., simulation #4) nonetheless overestimated membrane depolarization throughout the entire $[K^+]_o$ range in Fig. 19.

DISCUSSION

In cells, alterations to resting membrane potential and other homeostatic processes are addressed through a return to set values via complex cellular processing. For example, much like Hebbian synaptic plasticity, membrane potential itself is tightly regulated to maintain physiological conditions[24,25]. When self-regulation of these processes is no longer operating normally, pathological conditions can occur, though the exact effects of these changes are not known. Leak channels (e.g., K_{2p} and NALCN) play key roles in the maintenance of the electrochemical gradient. Unfortunately,

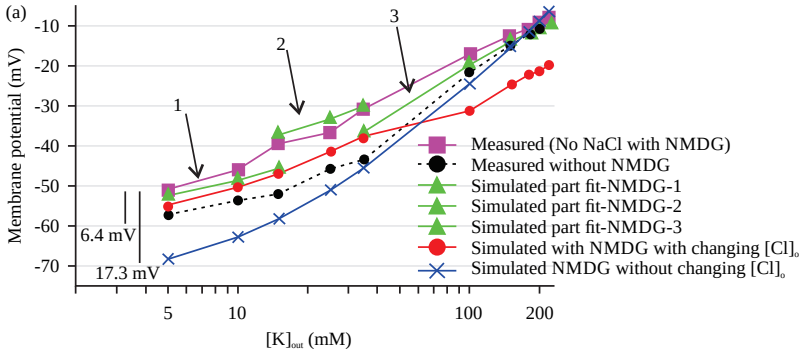

(b)

	a Partial Fit 1	b Partial Fit 2	c Partial Fit 3	d No Nacl Increase $[Cl]_o$ with KCl	e No NaCl No change $[Cl]_o$
pk	0.25	0.25	0.25	0.3	0.3
pNa	0.02	0.02	0.6	0.02	0.02
pC_i	0.45	0.2	0.2	0.45	0.45
$[K]_i$	140	140	140	140	140
$[Na]_i$	15	15	15	15	15
$[Cl]_i$	10	10	10	10	10
$[Na]_o$	10	10	10	10	10
$[Cl]_o$					110

(c)

$[Cl]_o$ Increase With KCL	$[K]_o$
21	0
26	5
31	10
36	15
46	25
56	35
121	100
171	150
201	180
221	200
241	220

Fig. 16(a-c): Measured and simulated relationships between membrane potential and increasing $[K^+]_o$ in m6m7>non-ORK1 larvae with and without NaCl/NMDG substitution, (a) Measured values with NaCl replaced by NMDG (purple line) compared to simulated values for the same condition (blue line) and for NaCl-containing saline (black dotted line), showing differences of 17.3 and 6.4 mV at 5 mM $[K^+]_o$, respectively. Additional simulations incorporating effects of rising $[Cl^-]_o$ and pCl from increased [KCl] are shown in red, (b) As no single simulation fit the entire dataset, three discrete segments (1, 2, and 3) were matched separately to empirical data, with parameter changes indicated in the legend (a-e) and (c) Saline $[Cl^-]_o$ values used in simulations a-d, showing variation as [KCl] increased

the regulation thereof is complex and it is not sufficient to know merely the expression profile of the cell (whether via RNA sequencing or other techniques for identifying mRNAs) due to the wide variety of possible channel subtypes and locations that could be involved[42,43]. Addressing the mechanisms behind the electrochemical gradient is thus an understandably monumental task, but utilization of a reductionist approach-that is, investigating the contributions of a single protein at a time-represents a manageable way to assemble a greater understanding of cell physiology.

Isolated cell cultures, cell lines, manipulated expression levels for *in vitro* and *in situ* studies and pharmacological agents can all be used to investigate the contributions of particular proteins to electrochemical gradients. Direct measures of membrane potential entail additional requirements for the experimental models used, as the external environment impacts how cells respond; no culture medium or "physiological saline" has yet mimicked the *in vivo* "internal milieu" entirely, though some have come close enough to allow measurement of differences between control cells and those with altered expressions in similar environmental conditions. Development of physiological saline to mimic the common salts within larval hemolymph[40] has provided a model by which *in situ* investigations can be conducted in *Drosophila*[44].

In this investigation, a K_{2p} channel subtype known to be endogenously present in *Drosophila* muscle (dORK1) was intentionally overexpressed in certain muscle cells and the response was investigated. While some adaptive compensation may have resulted in downstream effects, such as attempts to maintain a normal membrane potential through altered expression of other K_{2p} subtypes or decreased expression of the Na^+-K^+ pump, the results reported herein did not suggest that this was a major factor; membrane potential was observed to remain at a steady state of hyperpolarization in third instars developing with altered expression. It is possible that too great a degree of channel upregulation could alter homeostatic regulation[45]; attempts were made at controlling for this possibility through subsequent comparison with non-conducting K_{2p} expression (i.e., m6-m7>non-ORK1).

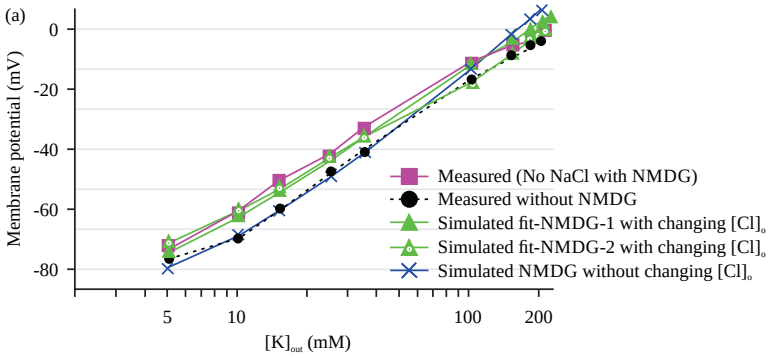

(b)

	a No NaCl Increase $[Cl]_o$ with KCL	b No NaCl Increase $[Cl]_o$ with KCL	c No NaCl No change $[Cl]_o$
pk	1.3	1.3	1.3
pNa	0.003	0.003	0.003
pC_i	0.6	0.8	0.8
$[K]_i$	140	140	140
$[Na]_i$	15	15	15
$[Cl]_i$	10	10	10
$[Na]_o$	10	10	145
$[Cl]_o$			110

(c)

$[Cl]_o$ Increase With KCL	$[K]_o$
21	0
26	5
31	10
36	15
46	25
56	35
121	100
171	150
201	180
221	200
241	220

Fig. 17(a-c): Measured and simulated relationships between membrane potential and rising $[K^+]_o$ in m6m7>ORK1 larvae with and without NaCl/NMDG substitution, (a) Values measured with exposure to salines containing NMDG in place of NaCl (purple line) were compared to simulated values for the same conditions (blue line) and for those measured in the presence of NaCl (black dotted line), respectively, with very small differences observed, (b) Additional simulations were conducted to consider the effects of rising $[Cl^-]_o$ and pCl from increasing [KCl] (green lines). The legend is labeled with a, b, and c to indicate the parameters used in the simulations and (c) Saline $[Cl^-]_o$ as KCl increases, as used in the simulations accounting for altered $[Cl^-]_o$ (simulations a-c)

The selective channel overexpression in muscles 6 and 7 allowed for comparison across the various skeletal muscles, though it was also observed to result in a high incidence of larval death[46]. The overexpression may also have resulted in altered function due to higher expression in organelle membranes within the muscle, as it is known that some K_{2p} channels are highly present in some organelle membranes[47]. Future studies examining overall mRNA expression differences between the m6/m7 muscles of m6-m7>non-ORK1 and m6-m7>ORK1 organisms, as well as unaltered muscles of the same larvae, would help determine whether overexpression alters the expression of other proteins. It would also be of interest to determine which of the 11 known *Drosophila* K_{2p} channel genes are normally expressed in identified cell types, as well as at what levels that expression takes place. The use of 10× Genomics or BD Rhapsody to examine these expression profiles in single cells may aid in such undertakings but is beyond the scope of this study[48].

The overall responses observed with m6m7>NA RNAi preparations exposed to the $[K^+]_o$ series were not any different from those observed with the parental lines (UAS-NA RNAi or UAS-Mid1 RNAi) or the m6m7>NA RNAi control muscle (m12). This could be due to low endogenous expression of NALCN in m6. An expression profile could be obtained if *in situ* hybridization for mRNA expression or immunocytochemistry for NALCN were available; however, such methods are not feasible for our study at this time, as no antibodies are available and our group is not primed for developing mRNA expression assays. However, we are hopeful that these physiological findings will complement future investigations.

The more hyperpolarized membrane potential observed in the m6m7>Mid1 RNAi strain was unexpected given that this response was different from that observed with the m6m7>NA RNAi strain despite the expected similarity of their profiles. This hyperpolarization could be explained if the Mid1 decrease resulted in NALCN reduction, but the RNAi NALCN reduction did not; additionally, Mid1 is associated with a wide

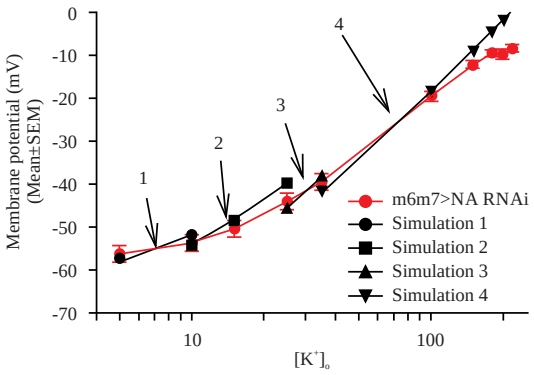

	Sim-1	Sim-2	Sim-3	Sim-4
pK	1.5	2	1	0.6
pNa	0.1	0.1	0.01	0.001
pC_l	0.45	0.45	0.45	0.45
$[K]_i$	140	140	140	140
$[Na]_i$	15	15	15	15
$[Na]_o$	145	145	145	145
$[Cl]_i$	10	10	10	10
$[Cl]_o$	110	110	110	110

Fig. 18: Measured and simulated relationships between membrane potential and altered $[K^+]_o$ in m6m7>NA RNAi larvae
Additional simulations were conducted to consider the effects of rising $[K^+]_o$ from increasing [KCl]. Given that no single simulation matched the measured values, four discrete, fragmented segments (1, 2, 3 and 4) were matched to the empirical data instead, with changes in the various parameters as shown. The legend is labeled with 1, 2, 3, and 4 to indicate the parameters used in the simulations and note that the best fits obtained involve gradual decreases in pK and pNa as KCl increases

array of channels in other models (i.e., yeast)[48], which might also be true in *Drosophila* as well. It would thus be of interest to determine whether the Mid1 RNAi strain affected (i.e., increased) expression of a functional K_{2p} channel to produce that hyperpolarization.

To address how a cell with K^+ leak channel overexpression responds to $[K^+]_o$ alterations, a series of acute $[K^+]_o$ increases was also investigated. As expected, cells overexpressing K_{2p} channels behaved like a K^+-sensitive electrode, with a linear response to raised $[K^+]_o$. This effect was also observed with $[K^+]_o$ alterations in the presence of NMDG, which suggests that ORK1 expression level is enough to dominate membrane potential even if NALCN are present. It would be expected that membrane potential would be close to E_K at rest given low $[K^+]_o$; however, it is estimated that the true E_K is around -90 mV[28,29] in larval muscle fibers and, even with K_{2p} channel overexpression and low $[K^+]_o$, the potential did not reach such large negative values. It should be noted that exposure to lipopolysaccharides (LPS) from *Serratia marcescens*, which transiently activate K_{2p} channels, with extracellular media devoid of Na^+ (0 mM KCl, 0 mM NaCl, 0 mM $NaHCO_3$, 80 mM NMDG) was observed to produce potentials as low as -100 mV in the same larval muscles in the m6-m7>ORK1 strain as studied herein[4]. These conflicting results imply that other channels, pumps, or exchangers may be contributing to the relative depolarization of the membrane potential from E_K observed herein.

Attempts to gain further insight using CP-96345 as a potential NALCN blocker were unsuccessful, as the effects were not significantly different from parental strains. Previous studies have investigated CP-96345, which is understood to block NALCN function in dopaminergic neurons, smooth muscle and bovine adrenal chromaffin cells[8,36,49-52] ; however, it has also been established that CP-96345- and the similarly structured L-703606- is more widely known as a Neurokinin 1 (NK1) receptor antagonist[7,36]. Since it has not been established whether CP-96345 selectively blocks NALCN in the absence of the NK1 receptor, we are reluctant to state that it selectively functions on *Drosophila* NALCN channels; this compound was only examined in this study due to feedback on an earlier study into the larval *Drosophila* heart[53]. This study found CP-96345 to have no effect on larval body wall muscle RMP, with DMSO exposure alone yielding a larger hyperpolarization than when used to dissolve the compound in m6m7>NA, whether examined in experimental (m6) or control (m12) muscles. In the strains used for examination of K_{2p} channel (ORK1) overexpression (i.e., m6m7>ORK1; non-conducting ORK1 m6m7>ORK1 NC; parental UAS-ORK1), CP-96345 had no effect.

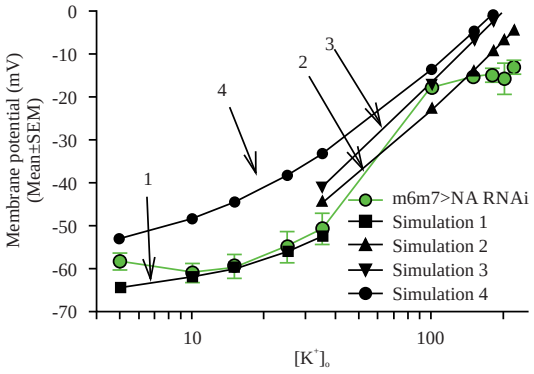

	Sim-1	Sim-2	Sim-3	Sim-4
pK	0.1	0.8	0.8	0.8
pNa	0.0001	0.001	0.00001	0.001
pC_l	0.45	1	0.45	0.45
$[K]_i$	140	140	140	140
$[Na]_i$	15	15	15	15
$[Na]_o$	145	145	145	145
$[Cl]_i$	10	10	10	10
$[Cl]_o$	110	110	110	110
pCa			0.001	
$[Ca]_i$			0.00001	
$[Ca]_o$			1	

Fig. 19: Measured and simulated relationships between membrane potential and altered $[K^+]_o$ in m6m7>Mid1 RNAi larvae
Additional simulations were conducted to consider the effects of rising $[K^+]_o$ from increasing [KCl]. Given that no single simulation matched the measured values, four discrete, fragmented segments (1, 2, 3 and 4) were matched to the empirical data instead, with changes in the various parameters as shown. The legend is labeled with 1, 2, 3 and 4 to indicate the parameters used in the simulations and note that a closer fit was observed when pK values increased and [KCl] was above 35 mM

To characterize ionic contribution to membrane potential in both control and ORK1-overexpressing cells, a reductionist approach was used, considering only K^+ and Na^+ permeabilities and estimating internal concentration values via the GHK equation. As in a previous study of Jan and Jan[27], it was determined that no set values of pK and pNa reliably predicted membrane potential perturbations for native muscle cells in larval *Drosophila*. To characterize the effects of RNAi-induced altered Mid1 expression on the membrane potential, simulations of the standard GHK equation parameters were used; however, as shown earlier[27], it is difficult to estimate the parameters for pNa, pK and pCa while achieving good fits with empirical data. Ion permeability does not seem to remain consistent, even with known external ion concentrations, good estimates of internal concentrations, and only a single variable (e.g., $[K^+]_o$) changing.

Estimates that pNa and pK decrease with altered $[K^+]_o$ appeared feasible for strains with linear responses to $[K^+]_o$ alteration, but the m6m7>Mid1 RNAi had had such a different relationship at low external $[K^+]_o$ as compared to higher external $[K^+]_o$ that such estimates did not produce a good fit for the empirical data (Simulation 4 in Fig. 19). Fragmented estimates over the full range of membrane potentials provided a better view of differences that could account for the potential contributions of various ions. Likely, the GHK equation's failure to predict membrane properties over a wide range of potentials is due to its inability to account for the various pumps and exchangers that also affect potential, as well as the fact that those proteins have varying contributions to membrane potential at different potentials[27]. Experimentally, attempts have been made at controlling other variables (such as the Na^+-K^+ pump and voltage-gated channels), but haven't been able to account for all the potential variables present in live cells. Considering that the Na^+-K^+ pump is electrogenic, no one parameter can be used to model its action over a range of potentials as it is greatly affected by membrane potential. Likewise, the ion exchanger function varies with shifts of the electrochemical gradient over a range of potentials.

As described above, the muscle fibers began contracting when $[K^+]_o$ reached 100 mM, which suggests either that voltage-gated Ca^{2+} channels opened or that the resulting depolarization was sufficient to provoke internal Ca^{2+} release from the sarcoplasmic reticulum (SER). *Drosophila* body wall muscles depend on voltage-gated Ca^{2+} channels in the plasma membrane for depolarization-induced muscle contraction[26].

The resulting influx of Ca^{2+} ions would also offset simulated estimates of the membrane potential obtained from the GHK equation, unless a pCa term was included, and with greater depolarization than the current parameter estimates would allow. The Ca^{2+} influx through voltage-gated Ca^{2+} channels would be expected to produce a rapid deflection towards depolarization, but this is not observed in the linear relationship empirically observed, suggesting that only a small amount of Ca^{2+} is needed to trigger contraction; however, such a small amount could not have produced such a large change in membrane potential. Reduction of Ca^{2+} influx could potentially be achieved by substitution with Ba^{2+} or Cd^{2+}, thus removing calcium from the bath, blocking that method of calcium entry and elucidating the involvement of Ca^{2+} in this phenomenon. However, earlier substitution of Cd^{2+} for Ca^{2+} resulted in both depolarization and contraction of the larval muscle[54] even though larval *Drosophila* skeletal muscle is known not to have a large sarcoplasmic reticulum (SER) due to the thin nature of its fibers, suggesting that Ca^{2+} flux from the Ca_V channels in the plasma membrane may be sufficient to achieve these results. It is known that Cd^{2+} can bind to troponin[31,32]; the results of the earlier studies might thus have been due to Cd^{2+} passing through Ca_V channels and binding to troponin, thereby inducing skeletal muscle contraction.

The potential that NALCN contributes to membrane dynamics was addressed herein by reducing the Na^+ driving gradient (0 mM NaCl) and replacing it with equal concentrations of NMDG (70 mM). Given that NMDG is commonly used as an equimolar substitution for Na^+ without harming cells[55], it was not expected to have other cellular effects; however, as $[Na^+]_o$ is reduced, it would be expected that the inward flux of sodium ions through NALCN would be reduced in turn, such that the membrane would be hyperpolarized as its potential is driven more towards the E_K. Interestingly, in salines for which the NaCl was replaced with NMDG, we noted that muscle contraction would start with the $[K^+]_o$ exchange around 25 mM, rather than the typical 100 mM, and excitatory junction potentials would appear as well, indicating that the motor nerve was being stimulated. This suggests that NMDG may have had a larger effect on the motor neurons than the muscle. However, the presence of NMDG resulted in a membrane potential trend opposite from that expected; rather than the expected hyperpolarization, depolarization was observed.

A few details could explain this discrepancy. It does appear that NMDG can pass through open-state voltage-gated K^+ channels (e.g., Kv3 channels)[56]. Given that K_{2p} channels, as leak channels, are constitutively open, NMDG may pass through them to enter the cell and depolarize the membrane. The K_{2p} channels may also be permeable to external Na^+ with low environmental pH (i.e., pH 6.0)[57]; however, this likely did not affect the results of these studies as pH was maintained at 7.2 throughout. It is also noted that NMDG produces a very rapid block of the BK_{Ca} channel from the inside of the membrane but not the outside[58], and blockage of the BKCa channel could partially account for the depolarized state observed here. However, this would likely occur at points wherein there is depolarization sufficient to open voltage-activated Ca^{2+} channels, at which values the effects of NMDG were observed to be reduced and NMDG was only applied via extracellular bathing media anyway, suggesting that this isn't the full explanation either. It should be noted that the simulations conducted to account for the depolarization induced by Na^+ removal in both m6m7>ORK1 and m6m7>non-ORK1 larvae did not fit well with parameters indicative only of an alteration in $[Na^+]_o$ and pNa; rather, multiple parameters needed altering to fit the empirical data. This suggests that there are likely ion channel effects of NMDG as yet unaccounted for in these larval muscles, though NMDG replacement alone does not provide good evidence of sodium-activated potassium currents[59]. Alternatively, choline chloride could be used to replace Na^+ to see whether similar responses are obtained. However, NMDG and choline chloride could have various actions on pumps and exchangers, as well requiring further investigations.

These findings have several potential implications for future studies. It is known that certain subtypes of K_{2p} channel bear altered expression in various cancerous tissues[60]; thus, targeting some channel subtypes (whether preferentially, acutely, or for prolonged periods) could aid in the development of selective tissue treatments. Additionally, as one determines the effects of altered expression for various K_{2p} subtypes and their responses to altered environmental conditions, one can better understand pathological processes at a physiological level.

Finally, it would be beneficial to investigate the precise nature and expression of K_{2p} channels in the muscle. These channels are present in the muscle throughout development, during which time the muscle undergoes a relatively rapid growth in surface area as it matures from embryo to third instar, yet it maintains relatively constant membrane potential and excitatory junction potential amplitude[61,62]. This suggests a very tight regulation of expression for proteins involved with membrane potential maintenance, about which we currently know very little. It would also be of interest to examine the effects of human pathological conditions on

channel expression levels, which could be performed through observation of various lines especially a GAL-80 heat-shock line at various points in the developmental timeline and subsequent exposure to acute environmental shifts that mimic such conditions (e.g., alterations to temperature or ionic balance).

CONCLUSION

Drosophila melanogaster with overexpression of conducting K_{2p} channels featured a more hyperpolarized resting membrane potential, greater potassium sensitivity and delayed contractions at higher potassium concentrations. The NA flies bearing knockdown of NALCN responded to potassium alterations in a way that resembled parental lines, possibly due to low endogenous m6 expression; however, Mid1 flies with knockdown of NALCN-associated proteins featured hyperpolarization similar to K_{2p} overexpressors.

SIGNIFICANCE STATEMENT

K_{2p} channels and NALCN are known to play very significant roles in the maintenance of resting membrane potential via the passive leak of potassium and sodium ions across the cell membrane; abnormal expression of these channels can thus result in very significant effects on the organism. By investigating the effects of some possible alterations to K_{2p} channel expression and NALCN expression in *Drosophila*, this experiment seeks to further elucidate the physiological effects thereof, as well as foster later experiments into the effects of K_{2p} and NALCN expression variation in other organisms.

ACKNOWLEDGMENT

This research was funded by the Beckman Scholars Program (E.R.E.) and Beckman mentor funds (R.L.C). Alumni of the research group (R.L.C.). Gatton Research Internship Grant (Y.K.).

REFERENCES

1. Goldstein, S.A.N., L.A. Price, D.N. Rosenthal and M.H. Pausch, 1996. ORK1, a potassium-selective leak channel with two pore domains cloned from *Drosophila melanogaster* by expression in *Saccharomyces cerevisiae*. Proc. Natl. Acad. Sci. U.S.A., 93: 13256-13261.
2. Lee, L.M., T. Müntefering, T. Budde, S.G. Meuth and T. Ruck, 2021. Pathophysiological role of K_{2P} channels in human diseases. Cell. Physiol. Biochem., 55: 65-86.
3. Elliott, E.R., A.C. Taul, M.O. Abul-Khoudoud, N. Hensley and R.L. Cooper, 2023. Effect of doxapram, a K2p channel blocker, and pH on heart rate: Larval *Drosophila* model. Appl. Biosci., 2: 406-420.
4. Hadjisavva, M.E. and R.L. Cooper, 2025. The biphasic effect of lipopolysaccharide on membrane potential. Membranes, Vol. 15. 10.3390/membranes15030074.
5. Lee, J.H., L.L. Cribbs and E. Perez-Reyes, 1999. Cloning of a novel four repeat protein related to voltage gated sodium and calcium channels. FEBS Lett., 445: 231-236.
6. Cochet-Bissuel, M., P. Lory and A. Monteil, 2014. The sodium leak channel, NALCN, in health and disease. Front. Cell. Neurosci., Vol. 8. 10.3389/fncel.2014.00132.
7. Monteil, A., N.C. Guérineau, A. Gil-Nagel, P. Parra-Diaz, P. Lory and A. Senatore, 2024. New insights into the physiology and pathophysiology of the atypical sodium leak channel NALCN. Physiol. Rev., 104: 399-472.
8. Ghezzi, A., B.J. Liebeskind, A. Thompson, N.S. Atkinson and H.H. Zakon, 2014. Ancient association between cation leak channels and Mid1 proteins is conserved in fungi and animals. Front. Mol. Neurosci., Vol. 7. 10.3389/fnmol.2014.00015.
9. Ren, D., 2011. Sodium leak channels in neuronal excitability and rhythmic behaviors. Neuron, 72: 899-911.
10. Lu, B., Y. Su, S. Das, J. Liu, J. Xia and D. Ren, 2007. The neuronal channel NALCN contributes resting sodium permeability and is required for normal respiratory rhythm. Cell, 129: 371-383.
11. Elliott, E.R. and R.L. Cooper, 2025. Fluoxetine antagonizes the acute response of LPS: Blocks K2P channels. Comp. Biochem. Physiol. C: Toxicol. Pharmacol., Vol. 287. 10.1016/j.cbpc.2024.110045.
12. Lear, B.C., E.J. Darrah, B.T. Aldrich, S. Gebre, R.L. Scott, H.A. Nash and R. Allada, 2013. UNC79 and UNC80, putative auxiliary subunits of the NARROW ABDOMEN ion channel, are indispensable for robust circadian locomotor rhythms in *Drosophila*. PLoS ONE, Vol. 8. 10.1371/journal.pone.0078147.
13. Liebeskind, B.J., D.M. Hillis and H.H. Zakon, 2012. Phylogeny unites animal sodium leak channels with fungal calcium channels in an ancient, voltage-insensitive clade. Mol. Biol. Evol., 29: 3613-3616.
14. Krishnan, K.S. and H.A. Nash, 1990. A genetic study of the anesthetic response: Mutants of *Drosophila melanogaster* altered in sensitivity to halothane. Proc. Natl. Acad. Sci. U.S.A., 87: 8632-8636.
15. Mir, B., S. Iyer, M. Ramaswami and K.S. Krishnan, 1997. A genetic and mosaic analysis of a locus involved in the anesthesia response of *Drosophila melanogaster*. Genetics, 147: 701-712.

16. van Swinderen, B., 2006. A succession of anesthetic endpoints in the *Drosophila* brain. J. Neurobiol., 66: 1195-1211.
17. Strohl, K.P., 2003. Periodic breathing and genetics. Respir. Physiol. Neurobiol., 135: 179-185.
18. Goldman, D.E., 1943. Potential, impedance, and rectification in membranes. J. Gen. Physiol., 27: 37-60.
19. Hodgkin, A.L. and B. Katz, 1949. The effect of sodium ions on the electrical activity of the giant axon of the squid. J. Physiol., 108: 37-77.
20. Maffeo, C., S. Bhattacharya, J. Yoo, D. Wells and A. Aksimentiev, 2012. Modeling and simulation of ion channels. Chem. Rev., 112: 6250-6284.
21. Marrink, S.J., V. Corradi, P.C.T. Souza, H.I. Ingólfsson, D.P. Tieleman and M.S.P. Sansom, 2019. Computational modeling of realistic cell membranes. Chem. Rev., 119: 6184-6226.
22. Gardner, C.L., W. Nonner and R.S. Eisenberg, 2004. Electrodiffusion model simulation of ionic channels: 1D simulations. J. Comput. Electron., 3: 25-31.
23. Liu, W., 2009. One-dimensional steady-state Poisson-Nernst-Planck systems for ion channels with multiple ion species. J. Differ. Equations, 246: 428-451.
24. Xie, D. and B. Lu, 2020. An effective finite element iterative solver for a Poisson--Nernst--Planck ion channel model with periodic boundary conditions. SIAM J. Sci. Comput., 42: B1490-B1516.
25. Hernandez, J., J. Fischbarg and L.S. Liebovitch, 1989. Kinetic model of the effects of electrogenic enzymes on the membrane potential. J. Theor. Biol., 137: 113-125.
26. Krans, J.L., K.D. Parfitt, K.D. Gawera, P.K. Rivlin and R.R. Hoy, 2010. The resting membrane potential of *Drosophila melanogaster* larval muscle depends strongly on external calcium concentration. J. Insect Physiol., 56: 304-313.
27. Jan, L.Y. and Y.N. Jan, 1976. Properties of the larval neuromuscular junction in *Drosophila melanogaster*. J. Physiol., 262: 189-214.
28. Ikeda, K., S. Ozawa and S. Hagiwara, 1976. Synaptic transmission reversibly conditioned by single-gene mutation in *Drosophila melanogaster*. Nature, 259: 489-491.
29. Salkoff, L.B. and R.J. Wyman, 1983. Ion currents in *Drosophila* flight muscles. J. Physiol., 337: 687-709.
30. Nitabach, M.N., J. Blau and T.C. Holmes, 2002. Electrical silencing of *Drosophila* pacemaker neurons stops the free-running circadian clock. Cell, 109: 485-495.
31. Flourakis, M., E. Kula-Eversole, A.L. Hutchison, T.H. Han and K. Aranda *et al*., 2015. A conserved bicycle model for circadian clock control of membrane excitability. Cell, 162: 836-848.
32. Campbell, D.B. and H.A. Nash, 1994. Use of *Drosophila* mutants to distinguish among volatile general anesthetics. Proc. Natl. Acad. Sci. U.S.A., 91: 2135-2139.
33. Leibovitch, B.A., D.B. Campbell, K.S. Krishnan and H.A. Nash, 1995. Mutations that affect ion channels change the sensitivity of *Drosophila melanogaster* to volatile anesthetics. J. Neurogenet., 10: 1-13.
34. Nash, H.A., R.L. Scott, B.C. Lear and R. Allada, 2002. An unusual cation channel mediates photic control of locomotion in *Drosophila*. Curr. Biol., 12: 2152-2158.
35. Hu, J., J. Han, H. Li, X. Zhang, L.l. Liu, F. Chen and B. Zeng, 2018. Human embryonic kidney 293 cells: A vehicle for biopharmaceutical manufacturing, structural biology, and electrophysiology: State of the art and future perspectives. Cells Tissues Organs, 205: 1-8.
36. Ferreira, J.J., C. Amazu, L.C. Puga-Molina, X. Ma, S.K. England and C.M. Santi, 2021. SLO2.1/NALCN a sodium signaling complex that regulates uterine activity. iScience, Vol. 24. 10.1016/j.isci.2021.103210.
37. Budnik, V., Y.H. Koh, B. Guan, B. Hartmann, C. Hough, D. Woods and M. Gorczyca, 1996. Regulation of synapse structure and function by the Drosophila tumor suppressor gene *dlg*. Neuron, 17: 627-640.
38. Sulkowski, M., Y.J. Kim and M. Serpe, 2013. Postsynaptic glutamate receptors regulate local BMP signaling at the *Drosophila* neuromuscular junction. Development, 141: 436-447.
39. Elliott, E.R. and R.L. Cooper, 2024. The effect of calcium ions on resting membrane potential. Biology, Vol. 13. 10.3390/biology13090750.
40. Stewart, B.A., H.L. Atwood, J.J. Renger, J. Wang and C.F. Wu, 1994. Improved stability of *Drosophila* larval neuromuscular preparations in haemolymph-like physiological solutions. J. Comp. Physiol. A., 175: 179-191.
41. de Castro, C., J. Titlow, Z.R. Majeed and R.L. Cooper, 2014. Analysis of various physiological salines for heart rate, CNS function, and synaptic transmission at neuromuscular junctions in *Drosophila melanogaster* larvae. J. Comp. Physiol. A, 200: 83-92.
42. Renigunta, V., G. Schlichthörl and J. Daut, 2015. Much more than a leak: Structure and function of K_{2P}-channels. Pflügers Arch. Eur. J. Physiol., 467: 867-894.
43. Niemeyer, M.I., L.P. Cid, W. González and F.V. Sepúlveda, 2016. Gating, regulation, and structure in K_{2P} K^+ channels: In *Varietate concordia*? Mol. Pharmacol., 90: 309-317.
44. Ashley, J. and R.A. Carrillo, 2024. The *Drosophila* larval neuromuscular junction: Developmental overview. Cold Spring Harbor Protoc., Vol. 2025. 10.1101/pdb.top108449.
45. Prelich, G., 2012. Gene overexpression: Uses, mechanisms, and interpretation. Genetics, 190: 841-854.
46. Elliott, E.R., K.E. Brock, R.M. Vacassenno, D.A. Harrison and R.L. Cooper, 2024. The effects of doxapram and its potential interactions with K2P channels in experimental model preparations. J. Comp. Physiol. A, 210: 869-884.

47. Zheng, C., J. Zheng, X. Wang, Y. Zhang, X. Ma and L. He, 2025. Two-pore-domain potassium channel Sandman regulates intestinal stem cell homeostasis and tumorigenesis in *Drosophila melanogaster*. J. Genet. Genomics, 10.1016/j.jgg.2025.05.003.
48. Iida, H., H. Nakamura, T. Ono, M.S. Okumura and Y. Anraku, 1994. *MID1*, a novel *Saccharomyces cerevisiae* gene encoding a plasma membrane protein, is required for Ca^{2+} influx and mating. Mol. Cell. Biol., 14: 8259-8271.
49. Gonzalez, J.C., H. Lee, A.M. Vincent, A.L. Hill and L.K. Goode *et al*., 2023. Circadian regulation of dentate gyrus excitability mediated by G-protein signaling. Cell Rep., Vol. 42. 10.1016/j.celrep.2023.112039.
50. Hahn, S., K.B. Um, S.W. Kim, H.J. Kim and M.K. Park, 2023. Proximal dendritic localization of NALCN channels underlies tonic and burst firing in nigral dopaminergic neurons. J. Physiol., 601: 171-193.
51. Um, K.B., S. Hahn, S.W. Kim, Y.J. Lee, L. Birnbaumer, H.J. Kim and M.K. Park, 2021. TRPC3 and NALCN channels drive pacemaking in substantia nigra dopaminergic neurons. eLife, Vol. 10. 10.7554/eLife.70920.
52. Yang, L., S. Pierce, T.W. Gould, G.L. Craviso and N. Leblanc, 2022. Ultrashort nanosecond electric pulses activate a conductance in bovine adrenal chromaffin cells that involves cation entry through TRPC and NALCN channels. Arch. Biochem. Biophys., Vol. 723. 10.1016/j.abb.2022.109252.
53. Taul, A.C., E.R. Elliott, D.A. Harrison and R.L. Cooper, 2025. The effects of overexpressing K2p channels in various tissues on physiology and behaviors. Insects, Vol. 16. 10.3390/insects16080787.
54. Potter, R., A. Meade, S. Potter and R.L. Cooper, 2021. Rapid and direct action of lipopolysaccharide (LPS) on skeletal muscle of larval *Drosophila*. Biology, Vol. 10. 10.3390/biology10121235.
55. Ting, J.T., B.R. Lee, P. Chong, G. Soler-Llavina and C. Cobbs *et al*., 2018. Preparation of acute brain slices using an optimized *N*-methyl-D-glucamine protective recovery method. J. Visualized Exp., Vol. 132. 10.3791/53825.
56. Wang, Z., N.C. Wong, Y. Cheng, S.J. Kehl and D. Fedida, 2009. Control of voltage-gated K^+ channel permeability to $NMDG^+$ by a residue at the outer pore. J. Gen. Physiol., 133: 361-374.
57. Ma, L., X. Zhang, M. Zhou and H. Chen, 2012. Acid-sensitive TWIK and TASK two-pore domain potassium channels change ion selectivity and become permeable to sodium in extracellular acidification. J. Biol. Chem., 287: 37145-37153.
58. Lippiat, J.D., N.B. Standen and N.W. Davies, 1998. Block of cloned BK_{Ca} channels (*rSlo*) expressed in HEK 293 cells by *N*-methyl D-glucamine. Pflügers Arch., 436: 810-812.
59. Thuma, J.B. and S.L. Hooper, 2018. Choline and NMDG directly reduce outward currents: Reduced outward current when these substances replace Na^+ is alone not evidence of Na^+-activated K^+ currents. J. Neurophysiol., 120: 3217-3233.
60. Williams, S., A. Bateman and I. O'Kelly, 2013. Altered expression of two-pore domain potassium (K_{2P}) channels in cancer. PLoS ONE, Vol. 8. 10.1371/journal.pone.0074589.
61. Li, H. and R.L. Cooper, 2001. Effects of the ecdysoneless mutant on synaptic efficacy and structure at the neuromuscular junction in *Drosophila* larvae during normal and prolonged development. Neuroscience, 106: 193-200.
62. Li, H., X. Peng and R.L. Cooper, 2002. Development of *Drosophila* larval neuromuscular junctions: Maintaining synaptic strength. Neuroscience, 115: 505-513.